Magnetoelectric effects in an organometallic quantum magnet

V. S. Zapf, P. Sengupta, C. D. Batista, F. Nasreen, F. Wolff-Fabris, and A. Paduan-Filho

Magnetoelectric effects in an organo-metallic quantum magnet

V. S. Zapf[1], P. Sengupta[2], C. D. Batista[3], F. Nasreen[1,4], F. Wolff-Fabris[1,†] and A. Paduan-Filho[5]

[1]*NHMFL, Los Alamos National Lab (LANL),*
Los Alamos, NM 87545, USA
[2]*Nanyang Technological University, Singapore 639798*
[3]*Theoretical Division, LANL,*
Los Alamos, NM 87545, USA
[4]*New Mexico State University, Las Cruces, NM, USA*
[5]*Instituto de Fisica, Universidade de Sao Paulo, Brazil*
[†]*Now at Dresden Hochfeld Labor, Dresden, Germany*

Metal-organic materials (sometimes known as metal-organic frameworks or molecular magnets) are a new field in which to search for ferroelectricity and coupling between electricity and magnetism. We observe a magnetic field-induced change in the electric polarization, $\Delta \mathbf{P}(H)$, that reaches 50 $\mu C/m^2$ in single crystals of $NiCl_2\text{-}4SC(NH_2)_2$ (DTN). DTN forms a tetragonal structure that breaks inversion symmetry, with the electrically polar thiourea molecules $[SC(NH_2)]$ all tilted in the same direction along the c-axis. The field H induces canted antiferromagnetism of the Ni $S = 1$ spins between 2 and 12 T and our measurements show that the electric polarization increases monotonically in this range, saturating above 12 T. By modelling the microscopic origin of this magnetoelectric effect, we find that the leading contribution to $\Delta \mathbf{P}$ comes from the change in the crystal electric field, with a smaller contribution from magnetic exchange striction. The finite value of $\Delta \mathbf{P}$ induced by magnetostriction results from the polar nature of the thiourea molecules bonded to the Ni atoms, and it is amplified by the softness of these organic molecules.

Magnetoelectrics are compounds in which the magnetic and electric susceptibilities are coupled, i.e., magnetic fields can induce electric polarization, while electric fields can induce magnetic polarization[1]. Research in this field is motivated by the promise of new devices as well as improving the speed, energy-efficiency and size of existing circuits[2–4]. The magnetoelectric effect can be particularly large when either the magnetic or electric subsystem is ordered, leading to diverging magnetic or electric susceptibilities. In particular, multiferroic behavior is a current hot topic that attempts to exploit the large effects that can result from simultaneous long range ordering of the magnetic and electric polarizations[2,5–12]. However, there is currently a dearth of materials exhibiting strong magnetoelectric coupling or multiferroic behavior and most research to date in these fields, particularly in multiferroics, has focused on transition-metal oxides.

Thus the idea of using organic ferroelectrics combined with transition metal ions as a starting point has the potential to greatly expand the available number of multiferroic or magnetoelectric materials[13,14]. Ferroelectricity by itself is
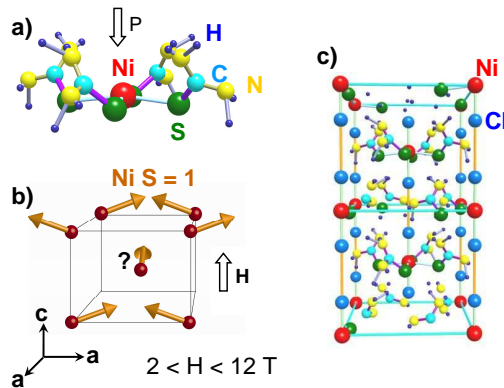

FIG. 1: Crystal structure of $NiCl_2\text{-}4SC(NH_2)_2$ (DTN) showing a) the thiourea coordination around the Ni ions and the likely direction of the electric polarization P, b) the canted frustrated antiferromagnetic structure of the Ni spins at intermediate fields between 2 and 12 T, and c) two unit cells of the full crystal structure.

known to occur in a number of organic molecules[15], and was most recently discovered above room temperature in croconic acid[16]. Organic materials usually possess soft lattice structures that could be easily modified by magnetic forces, leading to large magnetic field-induced changes in the electric polarization. In addition, the flexibility for designing organic molecules and the availability of electrically polar building blocks open many possibilities for building new magnetoelectric materials. A recent review of ferroelectricity in organic materials[15] has identified the electrically polar molecule thiourea, $SC(NH_2)_2$, as a strong candidate for organic ferroelectricity. In its crystalline form it is a ferroelectric with a T_c of 169 K and an electric polarization of 3,200 $\mu C/m^2$[17]. The origin of the electric polarization is primarily the polar double bond between carbon and the very electronegative sulfur atom. This bond is only partially compensated by the remainder of the molecule. In pure thiourea, the individual molecules are nearly but not quite anti-aligned, and an electric field can tilt the relative orientations, resulting in a ferroelectric response. Magnetism is also wide-spread in materials containing both organic components and transition-metal ions (variously known as metal-organics, organo-metallics, metal-organic frameworks, molecular magnets, or sometimes organic quantum magnets). In fact, magnetic order and ferroelectricity have been reported in the same material, although rarely coupled to each other.[13,14,18–21]

Here we show how magnetism can be combined with the electric properties of thiourea to produce strong magnetoelectric coupling, as evidenced by a magnetic field-induced change in electric polarization. We have performed experimental and theoretical investigations of the magnetoelectric properties of single crystals of $NiCl_2$-$4SC(NH_2)_2$ (DTN), which belongs to the polar point group I4 and is composed of four thiourea molecules bonded to each $NiCl_2$ unit. The Ni $S = 1$ moments occupy a tetragonal body-centered structure with antiferromagnetic interactions between nearest neighbors. The exchange coupling between the two interpenetrating tetragonal sublattices of Ni spins is very weak (smaller than 100mK) and frustrated. Consequently, we will neglect this coupling in the model Hamiltonian that is considered below. Any form of magnetostriction induces a change of the electric polarization, $\Delta\mathbf{P}$, because all the thiourea molecules are tilted in the same direction along the c-axis breaking spatial inversion symmetry (see fig. 1a).

DTN was previously investigated for magnetic field-induced quantum phase transitions that can be modeled in terms of Bose-Einstein Condensation of the magnetic spin system[22–31] and thus extensive information about its magnetic and magneto-elastic properties is available. The Hamiltonian of the magnetic system can be written as

$$\mathcal{H}_m = \sum_{\mathbf{r},\nu} J_\nu \mathbf{S}_\mathbf{r} \cdot \mathbf{S}_{\mathbf{r}+\mathbf{e}_\nu} + \sum_{\mathbf{r}} [D(S_\mathbf{r}^z)^2 - g\mu_B H S_\mathbf{r}^z], \tag{1}$$

Here $\mathbf{e}_\nu = \{a\hat{\mathbf{x}}, b\hat{\mathbf{y}}, c\hat{\mathbf{z}}\}$ are the relative vectors between nearest neighbor Ni ions, J_ν is the aniferromagnetic superexchange constants and g is the gyromagnetic ratio along the c-axis. D is a uniaxial anisotropy of the Ni spins of ~ 9 K that splits the Ni $\mathbf{S} = 1$ triplet into a $S^z = 0$ ground state and a $S^z = \pm 1$ excited doublet. The $S^z = 1$ state can be suppressed with applied magnetic fields along the tetragonal c-axis via the Zeeman effect until it becomes degenerate with the $S^z = 0$ state, thus producing a magnetic ground state above $H_{c1} = 2.1$ T. As shown in Fig. 2, antiferromagnetic super-exchange between the Ni spins produces long-range antiferromagnetic order in a dome-shaped region of the $T - H$ phase diagram between $H_{c1} = 2.1$ T, where the magnetic ground state is induced, and $H_{c2} \sim 12$ T where the spins align with the applied magnetic field[23]. The largest antiferromagnetic exchange occurs along the c-axis with $J_c = 2.2$ K. 3-D long-range order occurs below 1 K due to the weaker antiferromagnetic exchange along the a-axis with $J_a = 0.18$ K. The frustrated diagonal coupling is estimated to be less than 20 mK[26].

DTN shows significant spin-lattice coupling, which has been measured via magnetostriction[25] and sound velocity[29,30]. In effect, the Ni atoms attract each other along the c-axis when they are anti-aligned and their antiferromagnetic bonds are satisfied, and repel each other when they are aligned. This results in relative length changes of 10^{-4} since the lattice is relatively soft – the bulk modulus measured using resonant ultrasound spectroscopy is $E_{33} = 7.5 \pm 0.7$ GPa extrapolated to zero K[25], which is an order of magnitude smaller than typical inorganic metals and oxides.

Single crystals of DTN were grown from aqueous solutions of thiourea and nickel chloride. Two sets of samples were measured, one grown in an electric field $E = 50$ kV/m along the c-axis and the other in zero electric field. The idea was to determine whether growth in electric fields can influence the magnitude of the final electric polarization, either by modifying the structure or removing grain boundaries between regions with opposite c-axis orientation in this polar structure. The E-field grown sample had an electric polarization that was only 25% larger, and data on the E-field grown samples are presented. The change in electric polarization as a function of magnetic field $\Delta\mathbf{P}(\mathbf{H})$ was measured at temperatures down to 0.6 K with the samples immersed in liquid ^{3}He. Pulsed magnetic fields were employed at the National High Magnetic Field Laboratory (NHMFL) at Los Alamos National Laboratory. Data is shown from the down sweep of a relatively slow mid-pulse magnets at the NHMFL (~ 2000 T/s peak, 500 T/s average upsweep, 50 T/s average downsweep) to minimize magnetocaloric effects. Capacitor plates were constructed with a geometry that minimizes eddy currents, with Dupont silver paint on the faces of the single crystals perpendicular to
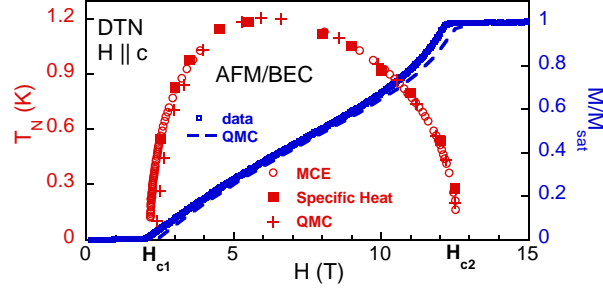
FIG. 2: Temperature T - Magnetic field H phase diagram for $H||c$ determined from specific heat and magnetocaloric effect (MCE) data, together with the result of Quantum Monte Carlo (QMC) simulations. The magnetization vs field measured at 16 mK and calculated from QMC is overlaid onto the phase diagram. The region of antiferromagnetism/Bose-Einstein Condensation (AFM/BEC) occurs under the red dome.[25]
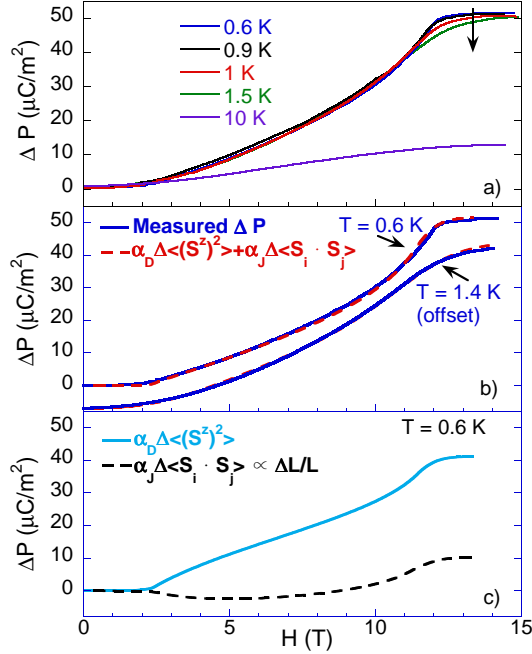

FIG. 3: a)The measured change in electric polarization $\Delta\mathbf{P} = \mathbf{P}(\mathbf{H}) - \mathbf{P}(0)$ as a function of magnetic field $\mathbf{H}$ for various temperatures between 0.6 and 10 K. The sign of $\Delta\mathbf{P}$ is unchanged under reversal of $\mathbf{H}$. b) $\Delta\mathbf{P}$ vs $\mathbf{H}$ at $T = 0.6$ K and 1.4 K compared to the fits (red dashed lines) to the expression $a_D\Delta\langle(S_z)^2\rangle + a_J\Delta\langle\mathbf{S_r} \cdot \mathbf{S_{r+e_c}}\rangle$ (see text) where the same values $a_D = 44.6\mu C/m^2$ and $a_J = 4.7\mu C/m^2$ are used for both fits. The expectation values are calculated by the Quantum Monte Carlo method at $T = 0.6$ K and 1.4 K. c) The individual terms $a_D\Delta\langle(S^z)^2\rangle$ and $a_J\Delta\langle\mathbf{S_r} \cdot \mathbf{S_{r+e_c}}\rangle$ at $T = 0.6$ K. Note that it was previously found that $\Delta\langle\mathbf{S_r} \cdot \mathbf{S_{r+e_c}}\rangle$ is proportional to the measured magnetostriction $\Delta L/L$ with $\mathbf{H}||\Delta L||\mathbf{e}_c$.[25]

the c-axis. The change in electric polarization $\Delta\mathbf{P}||\mathbf{H}||\mathbf{e_c}$ was measured with a Stanford Research 570 current-to-voltage amplifier. Dielectric constant measurements as a function of magnetic field were also performed capacitatively using a GC capacitance bridge driven at 30 V and 5 kHz with H and E along the c-axis. However no magnetic field-dependence of the dielectric constant could be resolved.

$\Delta\mathbf{P}(\mathbf{H}) = \mathbf{P}(\mathbf{H}) - \mathbf{P}(\mathbf{0})$ is shown in Fig. 3a for various temperatures. The data was taken after cooling the sample in zero electric and magnetic field, e.g. with no poling, and no change is observed if the sample is cooled in an electric field up to 0.2 MV/m. Essentially identical data with the same sign of $\Delta\mathbf{P}$ was found under reversal of the magnetic field, thus the coupling between the electric and magnetic polarization is bilinear in the magnetic moments, which for example is typical for magnetostrictive origins for the magneto-electric coupling. DTN is also a pyroelectric because it has a spontaneous polarization $\mathbf{P}$ in absence of electric field, that is not switchable without breaking the crystal structure (the electric ordering temperature is above the melting point of the crystal).

In determining the mechanism for the magnetoelectric coupling, we note that the two leading terms in the Hamil-

tonian are the single ion uniaxial anisotropy D of the Ni spins induced by the crystal electric fields of surrounding atoms, and the J_c exchange term along the c-axis. In a previous work we found that magnetic field-dependence of J_c was sufficient to account for the measured c-axis magnetostriction $\Delta L/L(\mathbf{H})$. Essentially the lattice deforms in an attempt to minimize the antiferromagnetic term of $\mathcal{H}_m$: $\sum_{\mathbf{r}} J_c \mathbf{S_r} \cdot \mathbf{S}_{\mathbf{r}+e_c}$. This was modelled by calculating the nearest-neighbor spin correlator $\langle \mathbf{S_r} \cdot \mathbf{S}_{\mathbf{r}+e_c} \rangle$ along the crystalline c-axis and noting that it is proportional to $\Delta L/L$, with the constant of proportionality containing details about the dependence of J_c on lattice spacing and the bulk modulus[25]. However, the magnetostriction has a non-monotonic magnetic field dependence whereas $\Delta \mathbf{P}(\mathbf{H})$ is monotonic. Thus we find that in order to properly model the observed $\Delta \mathbf{P}(\mathbf{H})$ we need to also take into account the D term in the Hamiltonian $\sum_{\mathbf{r}} D(S_{\mathbf{r}}^z)^2$.

To derive the expression for $\Delta P(H)$ we start by considering the free energy density of the lattice plus spin system as a function of the coordinates $\mathbf{r}_j$ $(1 \leq j \leq N)$ of the N different ions that constitute the unit cell of DTN: $f = f_L + f_M$, with

$$f_L = \sum_{j\mu,k\nu} \gamma_{j\mu,k\nu} r_j^\mu r_k^\nu, \tag{2}$$

$$f_M = -k_B T \ln\left[\text{Tr} e^{-\beta \mathcal{H}_m(\mathbf{r}_1,....,\mathbf{r}_N)}\right]. \tag{3}$$

Here k_B is the Boltzman constant and the greek indices μ, ν run over the three spatial components $\{x, y, z\}$. While f_L is a pure lattice contribution to the free energy density, f_M contains the coupling between the lattice and spin degrees of freedom. The coordinates $\mathbf{r}_j$ correspond to the ion displacements relative to the positions of equilibrium $\mathbf{R}_j$ *in absence of the spin degrees of freedom.* Since the magnetostrictive forces are much weaker than the elastic forces in DTN, we can safely assume that each ionic displacement is much smaller than the distances to the other ions: $|\mathbf{r}_j| \ll |\mathbf{R}_k - \mathbf{R}_j|$. This justifies the quadratic expansion of Eq.(2). The tensor $\gamma_{j\mu,k\nu}$ is hermitian and positively defined because we are expanding around the positions of equilibrium for $f_M = 0$. The Hamiltonian $\mathcal{H}_m$ depends on the coordinates $(\mathbf{r}_1, ..., \mathbf{r}_N)$ through the exchange and single-ion anisotropy parameters $J_c(\mathbf{r}_1, ..., \mathbf{r}_N)$ and $D(\mathbf{r}_1, ..., \mathbf{r}_N)$. We will neglect the dependence of J_a on the ionic coordinates because $|\partial J_a/\partial r_j^\nu| \ll |\partial J_c/\partial r_j^\nu|$.

The value of each coordinate r_k^ν is obtained by minimizing the free energy density as a function of the 3N coordinates r_j^μ: $\partial f/\partial r_j^\mu = 0 \ \forall \mu, j$. The result is:

$$r_k^\nu = -\sum_{j\mu} \eta_{k\nu,j\mu} \left[\frac{\partial J_c}{r_j^\mu} \langle \mathbf{S_r} \cdot \mathbf{S}_{\mathbf{r}+\mathbf{e}_c} \rangle + \frac{\partial D}{r_j^\mu} \langle (S_{\mathbf{r}}^z)^2 \rangle, \right] \tag{4}$$

where $\mathbf{r}$ is an arbitrary site of the lattice and $\eta_{k\nu,j\mu}$ are the components of the inverse of the tensor γ: $\sum_{j\mu} \eta_{k\nu,j\mu} \gamma_{j\mu,l\xi} = \delta_{kl}\delta_{\nu\xi}$. It is important to note that the derivatives $\frac{\partial D}{r_j^\mu}$ and $\frac{\partial J_c}{r_j^\mu}$ can be non-zero because the crystal has no inversion symmetry. By expanding the polarization to first order in the coordinates r_k^ν we obtain:

$$\mathbf{P} = \mathbf{P}_0 + \sum_{k\nu} \frac{\partial \mathbf{P}}{\partial r_k^\nu} r_k^\nu = \mathbf{P}_0 + a_J \langle \mathbf{S_r} \cdot \mathbf{S}_{\mathbf{r}+\mathbf{e}_c} \rangle + a_D \langle (S_{\mathbf{r}}^z)^2 \rangle, \tag{5}$$

with

$$a_J = -\sum_{k\nu,j\mu} \eta_{k\nu,j\mu} \frac{\partial \mathbf{P}}{\partial r_k^\nu} \frac{\partial J_c}{\partial r_j^\mu},$$

$$a_D = -\sum_{k\nu,j\mu} \eta_{k\nu,j\mu} \frac{\partial \mathbf{P}}{\partial r_k^\nu} \frac{\partial D}{\partial r_j^\mu}. \tag{6}$$

Since we do not have access to the microscopic parameters that appear in Eqs.(6), we will consider a_J and a_D as adjustable parameters that are determined by fitting $\Delta P(H)$.

The magnetic field and temperature dependence of the quantities $\langle (S^z)^2 \rangle$ and $\langle \mathbf{S}_i \cdot \mathbf{S}_j \rangle$ are calculated using quantum Monte Carlo (QMC) simulations of the Hamiltonian $\mathcal{H}_m$. We use the Stochastic Series Expansion (SSE) algorithm to simulate $\mathcal{H}_m$ on finite size systems. The SSE is a finite temperature QMC method[32] based on the importance sampling of the diagonal matrix elements of the partition function $e^{-\beta \mathcal{H}_M}$ expanded in a Taylor series. We used the previously measured parameters of the Hamiltonian[24], i.e., $J_c = 2.2$ K, $J_a = 0.18$ K, and $D = 8.6$ K. Simulations were performed on a tetragonal lattice of size $8 \times 8 \times 24$ and estimates of $\langle (S^z)^2 \rangle$ and $\langle \mathbf{S}_i \cdot \mathbf{S}_j \rangle$ along the c-axis were obtained. The results at 0.6K and 1.4 K are shown in Fig. 3b and c. We find indeed that the following expression

fits the experimental data at both temperatures: $\Delta P(H) = a_D \Delta \langle (S_{\mathbf{r}}^z)^2 \rangle + a_J \Delta \langle \mathbf{S_r} \cdot \mathbf{S_{r+e_c}} \rangle$. Here Δ indicates the change relative to the zero field value and a_J and a_D are adjustable parameters. The best fit to the data at $T = 0.6$ K yields $a_D = 44.6$ $\mu C/m^2$ and $a_J = 4.7$ $\mu C/m^2$. Significantly, these same parameters in combination with the $T=1.4$ K calculated values of $\langle (S^z)^2 \rangle$ and $\langle \mathbf{S_r} \cdot \mathbf{S_{r+e_c}} \rangle$ provide an excellent fit to the data at 1.4 K.

In terms of the microscopic mechanism, we note that in[25] it was suggested that the magnetostriction is due the Cl-Cl bonds in the Ni-Cl-Cl-Ni chains, which connect the individual $NiCl_2$-$4SC(NH_2)_2$ molecules to each other along the c-axis and are part of the antiferromagnetic superexchange pathway between Ni spins along the c-axis. The electric polarization however likely also contains a contribution from the off-center displacement of the Ni atom between the two Cl atoms, which would affect D, J_c, and the electric polarization. D is also affected by the four S atoms surrounding the Ni atom in the a-b plane and a distortion of these Ni-S bonds would have an amplified effect on the electric polarization due to the fact that the S atoms form the attachment point for the electrically polar thiourea molecule.

In conclusion, we observe a magnetoelectric effect of 50 $\mu C/m^2$ in the organo-metallic compound $NiCl_2$-$4SC(NH_2)_2$. This material addresses the challenge of not only combining electric and magnetic polarizations in one material, but also creating a strong coupling between them. In spite of the weak magnetic interactions, the size of $\Delta P(H)$ is comparable to or within a factor of 10 of other commonly-studied compounds with magnetic field-induced electric polarizations such as $TlCuCl_3$ and Ca_3MnCoO_6. This can be attributed to the softer nature of organic materials. A model of magnetic forces on the soft organic lattice from the single-ion and exchange terms of $\mathcal{H}_m$ provides an excellent fit to the data. The crystal structure of this material also intrinsically breaks spatial inversion symmetry, making it a type of ferroelectric with a transition temperature above the melting point of the crystal. This is the first example to our knowledge of the organic ferroelectric thiourea being used as a building block to create magnetoelectric behavior. Given the availability of thiourea and other organic ferroelectrics with relatively large ferroelectric polarizations and high ordering temperatures, coupled with the soft lattice structures of organo-metallic compounds, we propose this hybrid approach as an interesting area for further growth. The combination of stronger magneto-electric couplings and higher temperatures of the magnetic ordering are now a necessary step to further develop this field.

---

[1] M. Fiebig, J. Phys. D **38**, R123 (2005).

[2] S. Cheong and M. Mostovoy, Nature Materials **6**, 13 (2007).

[3] J. F. Scott, Nature Materials **6**, 256 (2007).

[4] Y. H. Chu et al., Nature Materials **7**, 478 (2008).

[5] T. Kimura et al., Nature **426**, 55 (2003).

[6] T. Goto, T. Kimura, G. Lawes, A. P. Ramirez, and Y. Tokura, Phys. Rev. Lett. **92**, 257201 (2004).

[7] N. Hur et al., Nature **429**, 392 (2004).

[8] G. Lawes et al., Phys. Rev. Lett. **95**, 087205 (2005).

[9] H. Katsura, N. Nagaosa, and A. V. Balatsky, Phys. Rev. Lett. **95**, 057205 (2005).

[10] M. Kenzelmann et al., Phys. Rev. Lett. **98**, 267205 (2007).

[11] T. Arima, J. Phys. Soc. Japan **76**, 073702 (2007).

[12] T. Kimura, Annu. Rev. Mater. Res. **37**, 387 (2007).

[13] V. S. Zapf, M. Kenzelmann, F. Wolff-Fabris, F. Balakirev, and Y. Chen (2010), arXiv:0904.4490v1.

[14] F. Kagawa, S. Horiuchi, M. Tokunaga, J. Fujioka, and Y. Tokura, Nature Physics **6**, 169 (2010).

[15] S. Horiuchi and Y. Tokura, Nature Materials **7**, 357 (2008).

[16] S. Horiuchi et al., Nature **463** (2010).

[17] G. J. Goldsmith and J. G. White, J. Chem. Phys. **31**, 1175 (1959).

[18] H.-B. Cui et al., J. Am. Chem. Soc. **128**, 15074 (2006).

[19] S. I. Ohkoshi et al., Angew. Chem. Int. Ed. **46**, 3238 (2007).

[20] P. Jain et al., J. Am. Chem. Soc. **131**, 13625 (2009).

[21] R. Ramesh, Nature **461**, 1218 (2009).

[22] A. Paduan-Filho, X. Gratens, and N. F. Oliveira. Jr., Phys. Rev. B **69**, 020405R (2004).

[23] V. S. Zapf et al., Phys. Rev. Lett. **96**, 077204 (2006).

[24] S. A. Zvyagin et al, Phys. Rev. Lett. **98**, 047205 (2007).

[25] V. S. Zapf et al., Phys. Rev. B **77**, R020404 (2008).

[26] S. A. Zvyagin et al., Phys. Rev. B **77**, 092413 (2008).

[27] L. Yin, J. S. Xia, V. S. Zapf, N. S. Sullivan, and A. Paduan-Filho, Phys. Rev. Lett. **101**, 187205 (2008).

[28] S. Cox, R. D. McDonald, M. Armanious, P. Sengupta, and A. Paduan-Filho, Phys. Rev. Lett. **101**, 087602 (2008).

[29] O. Chiatti et al., J. Phys. **150**, 042016 (2009).

[30] S. Zherlitsyn et al., J. Phys. **145**, 012069 (2009).

[31] A. Paduan-Filho, K. A. Al-Hassanieh, P. Sengupta, and M. Jaime, Phys. Rev. Letters **102**, 077204 (2009).

[32] A. W. Sandvik, Phys. Rev. B **59**, 14157(R) (1999).